J Therm Anal Calorim (2011) 103:443–451
DOI 10.1007/s10973-010-1094-0

Thermal degradation behavior of a carboxylic acid-terminated amphiphilic block copolymer poly(ethylene)-b-poly(ethylene oxide)

H. P. de Oliveira · J. Rieumont · C. Nogueiras ·
D. Souza · R. Sánchez

Received: 30 March 2010 / Accepted: 6 October 2010 / Published online: 20 October 2010

Abstract The thermal degradation of an amphiphilic block copolymer poly(ethylene)-b-poly(ethylene oxide)-carboxylic acid terminated (PE-b-80%PEO–CH_2COOH) and its salt obtained as intermediary product from chemical oxidation of the end group of poly(ethylene)-b-poly(ethylene oxide) (PE-b-80%PEO) has been studied using a thermogravimetric mass spectrometry (TG/MS) coupled system. The isothermal fragmentation of PE-b-80%PEO–CH_2COOH showed a more complex fragmentation pattern than PE-b-80%PEO owing to the simultaneous occurrence of the polyether block and the carboxylic end group fragmentations. This led to the appearance of four overlapping ion current peaks of fragments with *m*/*z* 44 and two peaks relative to *m*/*z* 18 at different times by acid-terminated copolymer. For the PE-b-80%PEO copolymer, two ion current peaks associated to *m*/*z* 44 and one large peak relative to *m*/*z* 18 fragments were detected. The intermediary product (PE-b-80%PEO–CH_2COO^- K^+) showed differences related to the fragmentation behavior. It has more defined ion current signals and presented characteristic peaks attributed to *m*/*z* 43 fragment at the very beginning of the thermal degradation process, which it not detected in the acid copolymer.

Keywords Thermal degradation · Amphiphilic copolymers · Chemical modification · Poly(ethylene)-b-poly(ethylene oxide) · Thermal stability · Mass spectrometric analysis

Introduction

Amphiphilic block copolymers are characterized by a hydrophobic block linked to a hydrophilic block by a covalent bond. These materials are interesting if applied as incompatible or heterogeneous blend in itself; since the role of the hydrophobic domains with respect to its overall properties is also worthy of further study. Because of these properties they have been used in the preparation of composites and compatibilizers in blends. Other interesting applications for amphiphilic block copolymers are their use as drug carriers [1–3], for drug solubilization [4, 5], micellar nanoencapsulation of fragrant [6], controlled release of drugs [7–11], and even for fullerenes encapsulation [12] are reported in literature. Thus, these materials have opened a new way for practical interest.

Furthermore, it is known that amphiphilic block copolymers can assemble in self-organized entities at nanolevel in aqueous solutions forming colloidal dispersions as well as in the molten state. Compared to common surfactant micelles, polymeric micelles of amphiphilic block copolymers are generally more stable having a remarkable lowered critical micellar concentration. These micelles have a fairly narrow size distribution and are characterized by a core–shell architecture, where the inner core is surrounded by a palisade of hydrophilic segments [13–17].

H. P. de Oliveira · J. Rieumont · C. Nogueiras
Colegiado de Pós-Graduação em Ciência dos Materiais,
Universidade Federal do Vale do São Francisco, 48902-300
Juazeiro, BA, Brazil

J. Rieumont · C. Nogueiras
Facultad de Química, Universidad de La Habana, Ciudad
Habana CP 10400, Cuba

D. Souza · R. Sánchez (✉)
Laboratórios de Materiais Avançados, Universidade Estadual do
Norte Fluminense, Campos dos Goytacazes 28013-602, RJ,
Brazil
e-mail: sanchez@uenf.br

Amphiphilic block copolymers are highly entangled and segment–segment interactions operate. Thus, thermal degradation of these materials can offer a real insight into such forces and in particular when chemical modification of one of the blocks is carried out.

Two main backbone scission mechanisms of thermal degradation of polymers [18] have been found: the so-called random chain scission and the terminal one or depolymerization. A third mechanism should be associated to the existence of alternating substituent groups in the polymer backbone that makes possible a chain of multiple consecutive eliminations. Major vinyl polymers, such as poly(vinyl chloride), poly(vinyl acetate), and poly(vinyl alcohol), degrade primarily by elimination of hydrochloric acid, acetic acid, and water, respectively [19, 20].

The first scission backbone mechanism one leads to a sudden decrease of the molecular mass because of the random break down of the polymer backbone giving rise to free radicals. They have high reactivity and participate in intermolecular chain transfer and disproportion termination. As a result, branched and cross-linked chains are formed and lead to the formation of a tar, as in the case of polyethylene. On the other hand, the mechanism releases the monomer molecules at the end of the polymer one by one through the formation of short free radicals of low reactivity, as is the case of poly(methylmethacrylate).

Thermal degradation and thermal oxidative degradation of poly(ethylene oxide) (PEO) have been studied [21, 22] producing ethylene and di-ethyl ether between other small molecules. Its thermal degradation was studied using different experimental methods, such as differential scanning calorimetry, thermogravimetry, and thermal volatilization analysis; the thermal degradation behavior of poly(ethylene oxide) blends with poly(vinylidenefluoride-*co*-hexafluoropropylene) for conductive applications [23] and with poly(L-lactic acid) [24] to the use in implants for bone repair was also studied.

The thermal degradation of poly(ethylene oxide) shows many features in common with its homologues poly(trimethylene oxide) and poly(tetrahydrofuran), with the main degradation processes being accounted by homolysis of the C–O backbone [25, 26]. The weakest bond in the backbone, and, therefore, the most susceptible to scission at lower temperatures, is the C–O bond (322 kJ mol^{-1}). However, for the C–C, the bond energy is 342 kJ mol^{-1}, a difference of 20 kJ mol^{-1} in bond strength implies that the bonds will undergo scission at comparable rates at 500 °C [27].

Thermal decomposition of poly(ethylene oxide) under non-oxidative conditions proceeds through one main step at 400 °C, point at which the main low-molecular mass degradation products were identified as ethyl alcohol, methyl alcohol, alkenes, ethoxymethane, ethoxyetane, methoxymethane, formaldehyde, acetaldehyde, ethylene oxide, water, CO, and CO_2 [28]. On the other side, thermal studies of acrylic polymers have pointed out that degradation begins with a water loss (dehydration) followed by a decarboxylation with CO_2 loss and chain scission at higher temperatures [29]. Another feature of this degradation is the appearance of the fragment *m*/*z* 73 as a rule. Thermal decomposition of poly (acrylic acid) and its salts has been thoroughly studied [30]. For the poly(acrylic acid), decarboxylation of anhydride becomes significant from about 250 °C, and there is a major fragmentation of the modified backbone from 300 °C. The alkali metal polyacrylates are more thermally stable polymers than poly(acrylic acid), degrading only above about 380 °C under programmed heating at 10 K min^{-1} [27, 31].

Interesting results were obtained by the thermal degradation of block copolymers. These copolymers showed similar thermal behavior with the corresponding homopolymers [32, 33]. One of these block copolymers, poly(ethylene)-b-poly(ethylene oxide) was chosen for the present study. This amphiphilic material can be functionalized to diversify the family of amphiphilic block copolymers and with them to find new properties and potentialities for their use as compatibilizers, intermediary in the synthesis of triblock copolymers, drug carrier matrix, composites, and so on.

By submitting PE-b-80%PEO to an oxidation process, the goal of the present study was to obtain a new copolymer PE-b-80%PEO–CH_2COOH, and to characterize the chemical modification by spectroscopic techniques and thermogravimentric analysis using a coupled mass spectrometry system.

Experimental

Materials

Poly(ethylene)-b-poly(ethylene oxide) with 20% PEO (PE-b-20%PEO), Aldrich, $M_n = 875$ g mol^{-1}, HLB = 4, poly(ethylene)-b-poly(ethylene oxide) with 50% PEO (PE-b-50%PEO), Aldrich, $M_n = 920$ g mol^{-1}, HLB = 10, $CMC = 28.8$ mg L^{-1} (25 °C), and poly(ethylene)-b-poly(ethylene oxide) with 80% PEO (PE-b-80%PEO) Aldrich, $M_n = 2250$ g mol^{-1}, were used as received.

Chemical modification of PE-b-80%PEO to terminal carboxylic acid copolymer (PE-b-80%PEO–CH_2COOH)

A colloidal dispersion of PE-b-80%PEO was oxidized by using a standard method [34] with potassium permanganate in alkaline solution. Taking into consideration this type of amphiphilic polymeric material, the procedure was modified to obtain PE-b-80%PEO–$CH_2COO^-K^+$. Subsequently, the carboxylic acid (PE-b-80%PEO–CH_2COOH) was obtained by reducing the pH. Carefully controlled centrifugation and filtration allowed to separate manganese dioxide particles from the dispersion of the copolymer. Total elimination of manganese dioxide particles was verified by optical microscopy. Final purification and drying of the obtained acid copolymer and its salt was carried out by dialysis and liofilization.

Characterization techniques

The Fourier transform infrared spectroscopy (FTIR) spectra were recorded in a FTIR Prestige 21-Shimadzu from 450 to 4500 cm^{-1} at a resolution of 1 cm^{-1}. Polymer samples were prepared on KBr pellets. Absorption spectra in the UV–Vis region were obtained using a Hach DR 5000 UV–Vis spectrometer, with quartz cells of 1 cm optical path.

Thermogravimetry and differential thermogravimetry analyses (TG–DTG) were carried out in dynamic conditions using thermogravimetric TA Instruments—SDT 2960, with thermobalance sensibility 0.1 µg. The analyses were conducted at a heating rate of 10 °C min^{-1}, in nitrogen atmosphere (100 mL min^{-1}) from 30 to 900 °C. The sample mass of the poly(ethylene)-b-poly(ethylene oxide), with different contents of the PEO block (20, 50, and 80%), were about 8 mg, which were placed in a platinum crucible.

The thermal fragmentation behavior of the PE-b-80%PEO and amphiphilic block copolymers with carboxylic acid terminated and the intermediary salt were analyzed. An on-line quadrupole mass spectrometer (Thermostar 200, Balzers Co.) synchronized with the thermobalance TA Instruments—SDT 2960 was used to analyze the pyrolytic exhaust gases produced by isothermal degradation of copolymers. The isothermal temperature (334 °C) was selected on basis of the dynamic analysis of the PE-b-80%PEO carboxylic acid terminated in helium atmosphere. Qualitative measurements of mass polymer fragments were obtained from the eluted gas of the thermal degradation process. After selection of the characteristic mass fragments, semi-quantitative measurements were obtained using multiple ion detection. Approximately 8 mg of samples in helium atmosphere (100 mL min^{-1}) were heated from room temperature at 20 °C min^{-1}, up to selected temperature and held for 30 min. The mass fragments of exhaust gases were measured by mass spectrometer with an ionization current of 90 V using a CH-TRON detector.

Results and discussion

Chemical modification of PE-b-80%PEO to terminal carboxylic acid copolymer (PE-b-80%PEO–CH_2COOH)

The chemical modification of PE-b-80%PEO to terminal carboxyl copolymer was carried out by oxidizing the hydroxyl terminal group of the PE-b-80%PEO ("Experimental" section). This reaction is heterogeneous because block copolymer forms a colloidal dispersion as previously commented. The chemical structure of the original polymer and their modifications are shown in the schematic representation of these blocks copolymers:

$$-(CH_2-CH_2)_{20}-(CH_2-CH_2-O)_{80}-CH_2CH_2OH\ \text{(pristine)}$$

$$-(CH_2-CH_2)_{20}-(CH_2-CH_2-O)_{80}-CH_2COO^-K^+$$

$$-(CH_2-CH_2)_{20}-(CH_2-CH_2-O)_{80}-CH_2COOH.$$

One of the crucial stages of the synthesis was the separation of the manganese dioxide particles produced during the reaction in the dispersion medium. Several techniques had to be used for an efficient separation including nanofilters.

Characterization of the PE-b-80%PEO–CH_2COOH and salt

The FTIR of the modified copolymer as potassium salt and carboxylic acid are shown in Fig. 1. For the copolymer as potassium carboxylate, the main new features in relation to the original copolymer are the signals at ν_s(OCO) 1640 cm^{-1} and ν_{as}(OCO) 1400 cm^{-1} [35] that can be assigned to the salt of the carboxylic acid, confirming the chemical transformation of the material. The intensity increase of the hydroxyl signal at $\nu_{(OH)}$ 3500 cm^{-1} can be explained by the high hygroscopicity of the carboxylic salts. Other main broad signals that appear forming part of

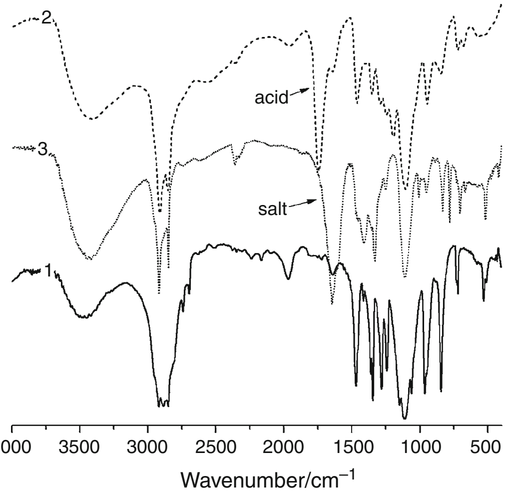

Fig. 1 FTIR spectra of the original copolymer PE-b-80%PEO (*1*) and modified copolymers (PE-b-80%PEO)–CH_2COOH (*2*) and (PE-b-80%PEO)–$CH_2COO^-\ K^+$ (*3*)

the initial polymer are νC–O–C ($\sim$1100 cm^{-1}) and C–H bending ($\sim$1340 cm^{-1}).

The main feature for the new copolymer with carboxylic acid end group is the presence of the signal corresponding to the carboxyl group stretching at 1740 cm^{-1} that appears on acidification of the copolymer as carboxylic salt. Other interesting feature for the copolymer as carboxylic acid end group is the stretching $\nu_{(OH)}$ at 3500 cm^{-1} and the CH stretching (around 2900 cm^{-1}) that appear separately. The association of carboxylic acids in dimmers is common in condensed phase [35] and polymers [36] and generally produces a broad band in the region 3300–3500 cm^{-1} (νOH) centered at 3000 cm^{-1}. Furthermore, the C=O stretching of dimmers appears between 1725 and 1680 cm^{-1}. All these dimmers signals are absent; thus, this peculiar feature shows that the carboxyl group is in this sample as an isolated end group. Other signals of these spectra are identical to the original polymer.

Colloidal dispersions

Aqueous dispersions of the copolymers PE-b-80% PEO, PE-b-80%PEO–CH_2COOH, and PE-b-80%PEO–$CH_2COO^-K^+$ were stable for several months indicating their colloidal character. UV–Vis spectra of diluted dispersions (Fig. 2) showed a maximum absorbance of PE-b-80%PEO at 191 nm, whereas for the copolymer salt, it is shifted to 202 nm and for the copolymer with carboxylic acid end group it was to 223 nm. The wavelength values are in accordance with the absorbance maximum of similar structures with such groups: C–O–C < COO^- < COOH. An additional characteristic of the new copolymer is that dispersions are formed faster than the non-modified copolymer, PE-b-80%PEO.

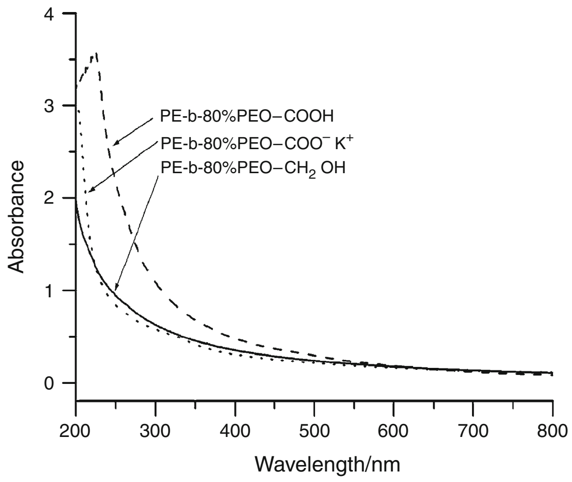

Fig. 2 UV spectra for diluted dispersions of PE-b-80%PEO, PE-b-80%PEO–CH_2COOH, and PE-b-80%PEO–CH_2COO^- K^+

Thermogravimetric analysis

Block copolymers without modification containing 20, 50, and 80% PEO were analyzed with the help of TG technique (Fig. 3) to compare them with the amphiphilic block copolymer synthesized in the present study. The TG curves for block copolymers in dynamic conditions (nitrogen atmosphere) showed that the mass loss occurs almost in an apparent single step. From the DTG curves of these block copolymers (Fig. 3), the structural impact of PEO contents on the thermal behavior could be observed with more clarity. Block copolymers with 50 and 80% of PEO had a thermal degradation window from 320 to 480 °C, but for PE-20%PEO copolymer, the temperature was shifted to 498 °C. The PE-b-80%PEO has a defined peak temperature (T_p) at 405 °C, PE-b-50%PEO showed a T_p at 400 °C and a shoulder at 410 °C, and the copolymer with a lower PEO content (20%) presented a T_p at 442 °C. This behavior is an indication that the polyethylene block is more prone to thermal degradation. The DTG curves definition and their T_p could clearly be correlated to PEO contents in the copolymers, since the block size had influence on the thermal behavior.

The thermal behavior of the PE-b-80%PEO and modified copolymers is shown in Fig. 4. The thermal stability of modified copolymers was reduced, maybe because a more efficient terminal mechanism of degradation is operating in this case, which should be associated to the effect of end group.

Helium as a carrier gas was used to define the degradation temperature for the isothermal study of copolymers. The comparative thermogram (Fig. 5) using helium and nitrogen as carrier gases shows that when helium was used as a carrier gas it could be detected different steps of the copolymer thermal degradation.

The derivative mass loss shows a shoulder at 294 °C and two relative defined peaks at 334 and 365 °C, respectively. Thus, it seems that fragmentations of the groups at the end of the chains probably occurs with the loss of small molecules such as water, CO_2, and short fragments, mainly

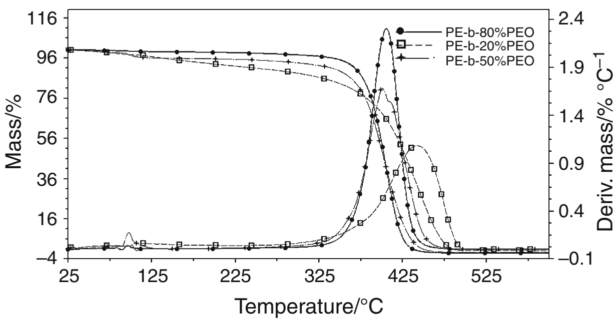

Fig. 3 TG–DTG curves of the block copolymers PE-b-PEO (20, 50, and 80% PEO) in nitrogen atmosphere

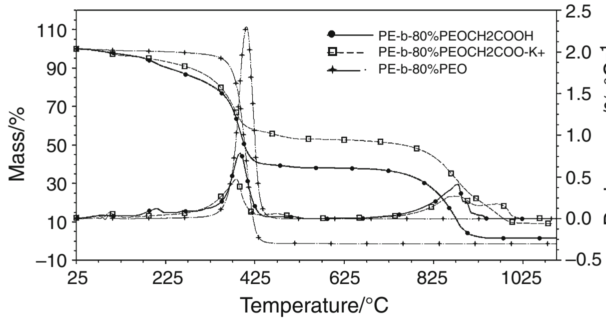

Fig. 4 Thermal stability (TG–DTG) of the PE-b-80%PEO, PE-b-80%PEO–CH_2COOH, and PE-b-80%PEO–CH_2COO^- K^+ copolymers

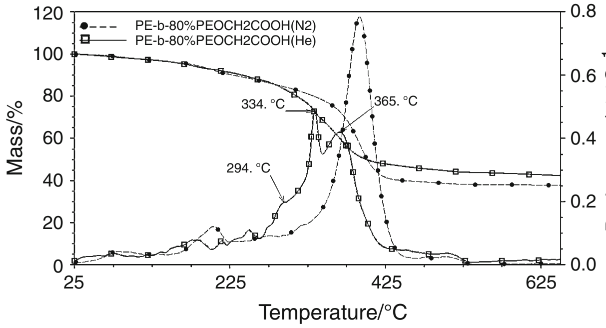

Fig. 5 TG–DTG curves of PE-b-80%PEO–CH_2COOH copolymer in helium atmosphere

from the carboxylic terminal and from hydroxyl end group of the polyether structure. They were followed by ruptures on the subsequent penultimate polymer segments at higher temperatures. A characteristic of this thermogram is that about 40% of the initial mass remains, it forms a tar that remains unchanged until 698 °C. It may be due to the existence of a cross-linked material produced during thermal degradation by a random breaking of C–C bonds.

Mass spectra results

Mass spectra of the PE-b-80%PEO–CH_2COOH at 294 and 365 °C

Mass spectra analysis of the carboxylic acid copolymer was carried out at isothermal conditions (294 and 365 °C). These temperatures were defined from previous non-isothermal analysis (Fig. 5). The results showed that the mass spectrum of PE-b-80%PEO–CH_2COOH at lower isothermal degradation temperature (294 °C) gave fragments with appreciable intensity up to *m*/*z* 60 although few fragments, with very small intensity, appear at greater *m*/*z* (Fig. 6). A significant contribution to ionic current of fragment *m*/*z* 44 (CO_2) appreciated at this temperature, which could have come from the decarboxylation process. Other important signals that could be associated to the end carboxylic structure of this copolymer were: *m*/*z* 18 (water); *m*/*z* 28 (C=O); *m*/*z* 32 (CH_3–OH); *m*/*z* 58 (OCH_2–CO); *m*/*z* 73 (CH_2 CH_2OCH_2–COH).

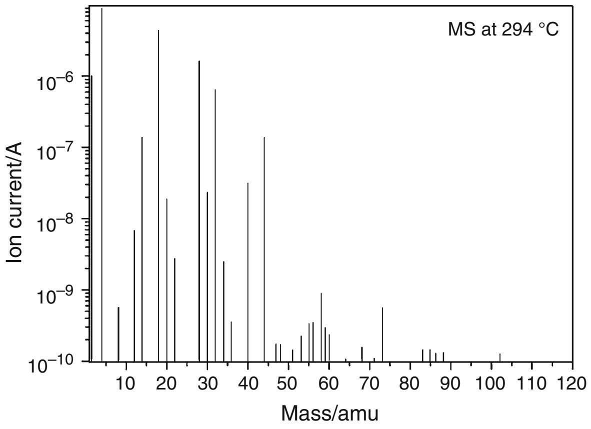

Fig. 6 Mass spectrum at the DTG peak temperature (294 °C) of PE-b-80%PEO–CH_2COOH copolymer

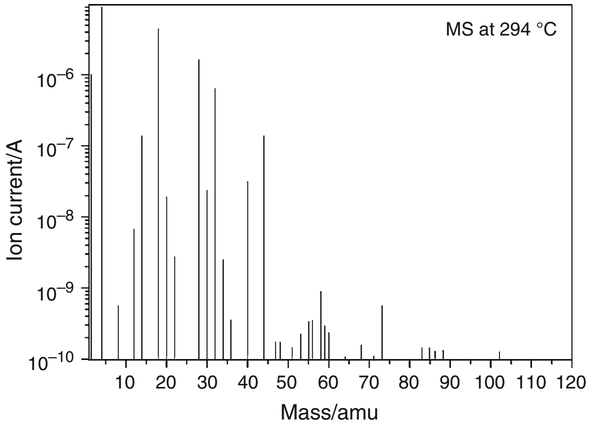

Fig. 7 Mass spectrum at the DTG peak temperature (365 °C) of PE-b-80%PEO–CH_2COOH copolymer

The isothermal degradation at higher temperature (365 °C) produced fragments with mass over *m*/*z* 60 and higher relative intensity (Fig. 7). These fragments were consequence to complex degradation mechanism that included scissions of the ether chain segment, in particular as ethylene oxide, such as *m*/*z* 88 ($CH_2CH_2OCH_2$–CH_2–O) and *m*/*z* 102 ($CH_2CH_2OCH_2$–CH_2–O–CH_2).

This thermal behavior is an evidence that degradation temperature required to the carboxylic end group is lower than the required by the ether chain. These facts indicate that in the carboxylic terminal copolymer, the fragmentation requires less energy to initiate the thermal decomposition.

Copolymers thermal fragmentation behavior during isothermal degradation at 334 °C

Homopolymer polyethylene thermal degradation occurs by random chain scission of the C–C linkage, whereas the polyethylene oxide thermal degradation is established by random homolysis scission of the C–C and C–O linkages [37]. The copolymer PE-b-80%PEO scissions and rearrangements gave a more complex fragmentation pattern than homopolymers (PE and PEO) but it preserved the characteristic fragmentation of each blocks**.**

The main difference that could be seen in PE-b-80%PEO related to modified polymers was because of the end groups in polyethylene oxide block. A comparative analysis of mass spectra data (Table 1) showed common relative abundant fragments with *m/z* 18, 28, 29, 43, and 44 and fragments with lower contribution, *m/z* 45, 54, 57, 73, and 86, but more significant for modified polymers.

Specific fragments of the acid and salt copolymers from the scission of the carboxylic end group were *m/z* 18, 28, 43, 44, 45, 57, and 73 and lower contribution of fragments with *m/z* equivalent to 18, 28, and so on, plus ethylene oxide units. These values are equal to those obtained from the thermal fragmentations of the ether block of copolymers. It is the reason from that the assignment of such fragments could not be done without ambiguity for the copolymer PE-b-80%PEO–CH_2COOH or its salt. However, by comparing the traces during the isothermal formation of the main fragments for the three materials under study shown in Figs. 8, 9, and 10, it was observed that

Table 1 Main *m/z* fragments to isothermal decomposition at 334 °C for the copolymers PE-b-80%PEO, PE-b-80%PEO–CH_2COOH, and PE-b-80%PEO–CH_2COO^- K^+

Frag. (*m/z*)	PE-b-80%PEO		PE-b-80%PEO–CH_2CO_2H		PE-b-80%PEO–CH_2C O_2^- K^+	
	Íon current/A	Peak time/min	Ion current/A	Peak time/min	Ion current/A	Peak time/min
18	5.0×10^{-7}	6.0	1.0×10^{-6}	4.0	1.0×10^{-6}	4.5
	–	–	1.2×10^{-7}	10.0	–	–
28	–	No peak	–	No peak	4.5×10^{-6}	8.5
29	2.0×10^{-8}	8.5	9.0×10^{-8}	8.5	7.5×10^{-8}	8.5
43	1.0×10^{-9}	8.5	2.0×10^{-8}	8.5	3.2×10^{-8}	2.0
	1.0×10^{-9}	3.5	2.1×10^{-8}	10.0	–	–
	–	–	5.0×10^{-9}	4.0	–	–
	–	–	6.0×10^{-9}	5.0	–	–
44	Weak	8.0	2.6×10^{-7}	4.0	1.5×10^{-6}	5.0
	Weak	3.5	2.7×10^{-7}	5.0	5.0×10^{-7}	8.5
	–	–	3.8×10^{-7}	9.0 (shoulder) 10.0	–	–
			4.0×10^{-7}			
45	2.5×10^{-9}	8.5	1.2×10^{-8}	9.0	1.3×10^{-8}	8.5
	Weak	Weak	1.1×10^{-8}	10.0	1.5×10^{-8}	5.0
	–	–	5.0×10^{-9}	5.0	–	–
54	No peak	No peak	6.0×10^{-10}	9.0 (shoulder)	1.0×10^{-9}	8.5
	–	–	1.0×10^{-9}	10.5	–	–
	–	–	Weak	5.5	–	–
57	Weak	8.5	1.5×10^{-9}	8.5	8.0×10^{-9}	8.5
	–	–	2.0×10^{-9}	10.5	–	–
71	6.0×10^{-10}	9.0	1.0×10^{-9}	9.0	–	–
	–	–	1.0×10^{-10}	5.0	–	–
73	4.0×10^{-10}	9.0	2.0×10^{-9}	9.0	2.8×10^{-9}	8.5
	–	–	1.6×10^{-9}	10.5	–	–
86	2.0×10^{-10}	9.0	5.0×10^{-10}	9.0	4.0×10^{-10}	9.0
	–	–	4.0×10^{-10}	10.5	–	–
89	–	–	1.0×10^{-10}	9.0	2.1×10^{-10}	9.0
	–	–	1.5×10^{-10}	11.0	–	–
102	–	–	4.0×10^{-10}	9.5	1.4×10^{-10}	9.0
	–	–	2.0×10^{-10}	5.5	–	–

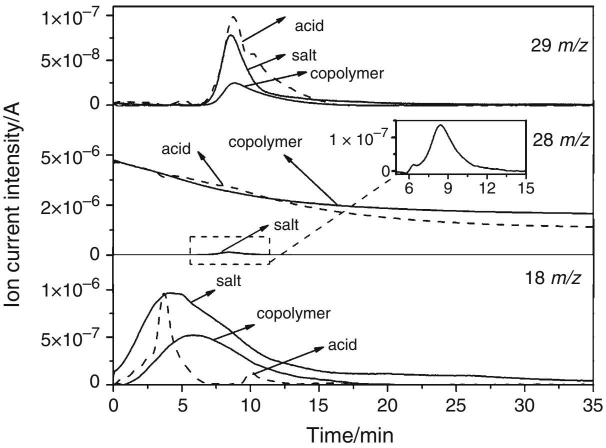

Fig. 8 Ion current curves (fragments *m/z* 18, 28, and 29) at 334 °C for the copolymers PE-b-80%PEO, PE-b-80%PEO–CH_2COOH, and PE-b- 80%PE-b-PEO–CH_2COO^- K^+

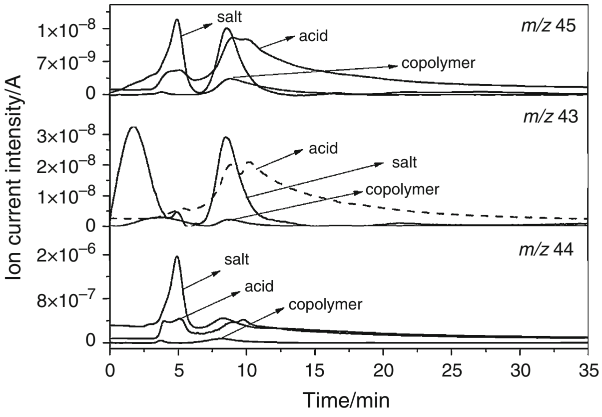

Fig. 9 Ion current curves (fragments *m/z* 43, 44, and 45) at 334 °C for the copolymers PE-b-80%PEO, PE-b-80%PEO–COOH, and PE-b-80%PEO–COO^- K^+

several differences appeared that justify the true origin of some fragments. It was seen that the higher ion current intensity appeared in the *m/z* 18, 28, 29, and 44 for modified copolymers and as a rule the PE-b-80%PEO presented the lower intensity of the peaks except for the *m/z* 18 and 44.

General characteristics of the copolymers fragmentations are seen in the fragments with *m/z* 18, 28, and 29 (Fig. 8). The isothermal formation of *m/z* 18 fragments for the PE-b-80%PEO related to water loss from ethylene block, gave a broad ion current peak around 5.5 min (Fig. 8). This signal *m/z* 18 for the salt copolymer presented a broad ion current peak too but before 5 min. However, from the acid copolymer, this signal was sharp at 4 min accompanied by a minor ion current peak at 9.5 min (Fig. 8 and Table 1). Thus, it suggests that for the acid copolymer the water was lost by a different mechanism.

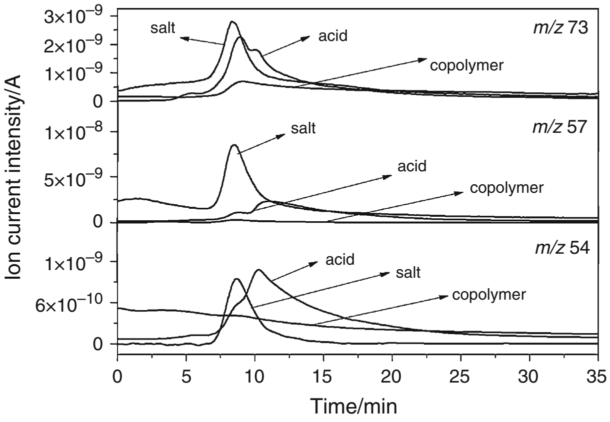

Fig. 10 Ion current curves (fragments *m/z* 54, 57, and 73) at 334 °C for the copolymers PE-b-80%PEO, PE-b-80%PEO–CH_2COOH, and PE-b-80%PEO–COO^- K^+

The fragment *m/z* 28 steadily decreases for the PE-b-80%PEO corresponding to the loss of CH_2–CH_2. The same trend is observed for the acid copolymer. However, this trace is very different from that observed for the salt copolymer (Fig. 8), which affords a sharp peak suggesting that this loss can also be related to the C=O loss. Signal *m/z* 29 is very similar to the three other materials presenting peaks at 9 min, which in the case of the acid copolymer is split twice. The intensity of the *m/z* 29 is higher for the salt and acid copolymers compared to PE-b-80%PEO. Although the signal *m/z* 28 could be associated to the C=O loss for the carboxylic copolymers, the signal *m/z* 29 probably could be related to the protonated C=O.

The ionic current intensity due to the fragments *m/z* 43, 44, and 45 are shown in Fig. 9. The ion current signals of these fragments, for the salt and acid copolymer, showed two peaks for each fragment and one peak for the copolymer PE-b-80%PEO. These peaks appeared at two times, at 4.5 and 8 min, indicating that these fragments have different origins, associated to two types of fragmentations. These fragments could be associated to the loss of a CO_2 group from the carboxylic copolymers or to the fragment CH_2CH_2O from the ethylene oxide block giving in both cases the *m/z* 44. Furthermore, the peaks for the acid copolymer are split giving double peaks.

At lesser time (4.5 min), ion current peaks appear because of fragments *m/z* 44 and 45 but not for the fragment *m/z* 43 (Fig. 9). These peaks are observed in the salt and acid copolymers but not in the PE-b-80%PEO. This feature means that these fragments correspond to a process of decarboxilation, which could not arise from the PE-b-80%PEO. This is in agreement with the feature for the modified copolymer, acid, and salt; the formation of a signal at *m/z* 43 is not possible because the fragment *m/z* 44 is essentially CO_2 that cannot lose a proton and become an *m/z* 43 fragment.

The second peak at around 8 min because of fragments *m*/*z* 43, 44, and 45, was weak when compared with the PE-b-80%PEO, and undoubtedly they would correspond to the fragment CH_2CH_2O of the ether block. The difference in the intensity of the signals *m*/*z* 43 and 45 are related to the gain or loss of a proton from ion *m*/*z* 44. However, for the *m*/*z* 43 of the salt copolymer, the first peak appears at a position of 2 min before giving a little intermediate peak at the same position (4.5 min) than for the *m*/*z* 44 and *m*/*z* 45. It suggests that the salt copolymer is able to give the fragment CH_2–C=OH of *m*/*z* 43 from the carboxylate; however, for the acid copolymer fragmentation is not possible. This result indicates clearly the difference in fragmentation pattern between the salt and the acid copolymer.

Ion current because of traces of fragments with *m*/*z* 73, 57, and 54 are shown in Fig. 10. These signals were weak or they do not appear for the PE-b-80%PEO isothermal degradation, which were comparatively more intense for the acid and salt copolymers. This is an indication that these fragments come from the resting carboxylic moiety of these copolymers. The fragments *m*/*z* 57 seem to come from O–CH_2–CH_2–C=O or CH_2–COO and OCH_2–COO for the *m*/*z* 73. The intensity of the peak *m*/*z* 57 for the salt copolymer is much more intensive than that for the acid copolymer. The appearance of fragment *m*/*z* 54 could not be assigned and steadily decreases for the PE-b-80%PEO copolymer, in contrast to the other polymers.

Conclusions

A novel amphiphilic block copolymer was obtained by oxidizing the hydroxyl terminal group of PE-b-80%PEO to produce PE-b-80%PEO–CH_2COOH with carboxylic acid end group and its potassium salt as an intermediary. Both the materials were characterized by spectroscopic methods, infrared, ultraviolet, and mass spectrometry. These compounds formed stable colloidal dispersions in water for several months. The PE-b-80%PEO–CH_2COOH copolymer had shown less thermal stability than its salt and the PE-b-80%PEO block copolymers. Furthermore, the carboxylic acid copolymer offered a complex thermal fragmentation pattern because these copolymer thermal degradation reactions simultaneously take place on the carboxylic moiety and on the polyether chain.

References

1. Kataoka K, Harada A, Nagasaki Y. Block copolymer micelles for drug delivery: design, characterization and biological significance. Adv Drug Deliv Rev. 2001;47:113–31.
2. Gaucher G, Dufresne MH, Sant VP, Kang N, Maysinger D, Leroux JC. Block copolymer micelles: preparation, characterization and application in drug delivery. J Controlled Rel. 2005;109:169–88.
3. Rosler A, Vander meulen GWM, Klok HA. Advanced drug delivery devices via self-assembly of amphiphilic block copolymers. Adv Drug Deliv Rev. 2001;53:95–108.
4. Nagarajan R, Barry M, Ruckenstein E. Unusual selectivity in solubilization by block copolymer micelles. Langmuir. 1986;2(2):210–5.
5. Velluto D, Demurtas D, Hubbell JA. PEG-b-PPS diblock copolymer aggregates for hydrophobic drug solubilization and release: cyclosporin A as an example. Mol Pharm. 2008;5(4):632–42.
6. Ternat C, Kreutzer G, Plummer CJG, Christopher JG, Nguyen TO, Herrmann A, Ouali L, Sommer H, Fieber W, Velazco MI, Klok HA, Manson JAE. Amphiphilic multi-arm star-block copolymers for encapsulation of fragrance molecules. Macromol Chem Phys. 2007;208(2):131–45.
7. Adams DJ, Adams S, Atkins D, Butler MF, Furzeland S. Impact of mechanism of formation on encapsulation in block copolymer vesicles. J Controlled Rel. 2008;128:165–70.
8. Tian Z, Wang M, Zhang A, Feng Z. Preparation and evaluation of novel amphiphilic glycopeptide block copolymers as carriers for controlled drug release. Polymer. 2008;49(2):446–54.
9. Qiu LY, Zhang JX, Yan MQ, Jin Y, Zhu KJ. Reverse self-assemblies based on amphiphilic polyphosphazenes for encapsulation of water-soluble molecules. Nanotechnology. 2007;18(47):475602.
10. Lin XN, Zhou RM, Qiao Y, Jin FM, Zhai YL, Xing JF, Deng LD, Dong AJ. Poly(ethylene glycol)/poly(ethyl cyanoacrylate) amphiphilic triblock copolymer nanoparticles as delivery vehicles for dexamethason. J Polym Sci Part A Polym Chem. 2008;46(23):7809–15.
11. Wu Y, Che FB, Chen JH. Synthesis and characterization of a amphiphilic pluronic-poly(D,L-lactide-co-glycolide) copolymer and their nanoparticles as protein delivery systems. J Appl Polym Sci. 2008;110(2):1118–28.
12. Chen L, Jenekhe SA. Solubilization and encapsulation of fullerenes by amphiphilic block copolymers. Langmuir. 1999;15(23):8007–17.
13. Moffitt M, Khougaz K, Eisenberg A. Micellization of ionic block copolymers. Acc Chem Res. 1996;29(2):95–102.
14. Lanson D, Schappacher M, Borsali D, Deffieux A. Poly(styrene)comb-b-poly(ethylene oxide)comb copolymers: synthesis and AFM investigation of intra and supramolecular organization as thin deposits. Macromolecules. 2007;40(26):5559–65.
15. Soo PL, Eisenberg A. Preparation of block copolymer vesicles in solution. J Polym Sci Part B Polym Phys. 2004;42(6):923–38.
16. Wang D, Peng Z, Liu X, Tong Z, Wang C, Ben B. Synthesis and micelle formation of triblock copolymers poly(methylmethacrylate)-b-poly(ethylene oxide)-b-poly (methylmethacrylate) in aqueous solution. Eur Polym J. 2007;43(7):2799–808.
17. Hajduk DA, Kossuth MB, Hillmyer MA, Bates FS. Complex phase behavior in aqueous solutions of poly(ethylene oxide)-poly(ethylene) block copolymers. J Phys Chem B. 1998;102:4269–76.
18. Billmeyer FW. Textbook of polymer science. New York: Wiley; 1984.
19. Ivan B, Kennedy JP, Kelen T, Tüdõs F, Nagy TT, Turcsányi B. Degradation of PVCs obtained by controlled chemical dehydrochlorination. J Polym Sci (Polymer Chemistry Edition). 1983:2177–88.
20. Ivan B, Turcsányi B, Kelen T, Tüdõs F. Thermooxidative degradation of PVC in solution in the presence of metal stearate stabilizers. Die Angew Makromol Chem. 1991;189(1):35–49.
21. Fares MM, Hacaloglu J, Suzer S. Characterization of degradation products of poly(ethylene oxide) by pyrolysis mass-spectroscopy. Eur Polym J. 1994;30(7):845–50.

22. Yang L, Heatley F, Blease TG, Thompson RIG. A study of the mechanism of the oxidative thermic degradation of poly(ethylene oxide) and poly(propylene oxide) using H^1 and C^{13} NMR. Eur Polym J. 1996;32(5):535–47.
23. Malik P, Castro M, Carrot C. Thermal degradation during melt processing of poly(ethylene oxide), poly(vinylidene fluoride-co-hexafluro propylene) and their blends in presence of additives for conducting applications. Polym Degrad Stab. 2006;91(4):634–40.
24. Zoppi RA, Duek EAR, Coraça DC, Barros PP. Preparation and characterization of poly(L-lactic acid) and poly(ethylene oxide) blends. Mater Res. 2001;4:117–25.
25. Uyar T, Hacaloglu J. Thermal degradation of poly(propylene oxide) and polyepichlorohydrin by direct mass spectrometry. J Anal Appl Pyrolysis. 2002;64:379–93.
26. Costa L, Luda MP, Cameron GG, Qureshi MY. The thermal and thermo-oxidative degradation of poly(tetrahydrofuran) and its complexes with LiBr and LiI. Polym Degrad Stab. 2000;67: 527–33.
27. McNeill IC, Sadeghi SMT. Thermal stability and degradation mechanisms of poly(acrylic acid) and its salts.2. Sodium and potassium salts. Polym Degrad Stab. 1990;30(2):213–30.
28. Pielichowski K, Flejtuch K. Non-oxidative thermal degradation of poly(ethylene oxide): kinetic and thermoanalytical study. J Anal Appl Pyrolysis. 2005;73:131–8.
29. Latimer RP. Pyrolysis mass spectrometry of acrylic polymers. J Anal Appl Pyrolysis. 2003;68–69:3–14.
30. McNeill IC, Sadeghi SMT. Thermal stability and degradation mechanisms of poly(acrylic acid) and its salts.1. Poly(acrylic acid). Polym Degrad Stab. 1990;29(2):233–46.
31. McNeill IC, Alston A. Thermal degradation behaviour of acrylic salt polymers and ionomers. Die Angew Makromol Chem. 1998;261(262):157–72.
32. Hacaloglu J, Fares MM, Suzer S. Pyrolysis mass spectrometric analysis of styrene-isoprene-styrene copolymers. Eur Polym J. 1999;35:939–44.
33. Hacaloglu J, Ersen T, Ertugrul N, Fares MM, Suzer S. Pyrolysis mass spectrometric analysis of styrene-butadiene block and random copolymers. Eur Polym J. 1997;33(2):199–203.
34. Furniss BS, Hannaford AJ, Smith PWG, Tatchell AR. Vogel's textbook of practical organic chemistry. 5th ed. London, UK: Longman; 1989. p. 668.
35. Smith BC. Fourier transform infrared spectroscopy. Boca Raton, FL: CRC Press; 1996.
36. Berthold J, Desbrieres J, Rinaudo M, Salman L. Types of adsorption water in relation to the ionic groups and their counter ions for some cellulose derivatives. Polymer. 1994;35(26): 5729–36.
37. Han X, Hu YH, Lin ZK, Li SF, Zhao FQ, Liu ZR, Yi JH, Zhang LY, Ren XN. Effects of fullerenes on thermal behaviors of polyethylene glycol. J Therm Anal Calorim. 2008;93(3):927–32.